

Electronic and transport properties of reduced and oxidized nanocrystalline TiO₂ films

A. Rothschild^{a)} and Y. Komem

Faculty of Materials Engineering, Technion, Haifa 32000, Israel

A. Levakov, N. Ashkenasy,^{b)} and Yoram Shapira

Department of Electrical Engineering, Tel Aviv University, Tel Aviv 69978, Israel

(Received 6 September 2002; accepted 29 November 2002)

Electronic properties of reduced (vacuum-annealed) and oxidized (air-annealed) TiO₂ films were investigated by *in situ* conductivity and current–voltage measurements as a function of the ambient oxygen pressure and temperature, and by *ex situ* surface photovoltage spectroscopy. The films were quite conductive in the reduced state but their resistance drastically increased upon exposure to air at 350 °C. In addition, the surface potential barrier was found to be much larger for the oxidized versus the reduced films. This behavior may be attributed to the formation of surface and grain boundary barriers due to electron trapping at interface states associated with chemisorbed oxygen species. © 2003 American Institute of Physics. [DOI: 10.1063/1.1539556]

Nanocrystalline titanium dioxide (TiO₂) has many important applications, such as solar cells,¹ photocatalysts for water photolysis² and degradation of environmental pollutants in air and wastewaters,³ as well as an oxygen- and a gas-sensor material.⁴ Thin films of TiO₂ prepared by reactive sputtering for gas-sensing applications were found to crystallize to a dense columnar layer of nanocrystalline rutile upon annealing at 400 °C.⁵ Their electrical conductivity was quite sensitive to changes in the ambient oxygen pressure between 200 and 325 °C. Analysis of the response kinetics during exposure of reduced TiO_{2- δ} films to oxygen indicated that it could be explained by a twofold mechanism: First, oxygen is chemisorbed at the surface, producing a depletion layer in the adjacent space-charge region, and subsequently follows oxidation of the entire film and annealing of donor-like oxygen vacancies by grain-boundary-enhanced chemical diffusion.⁶

Chemisorption of oxygen builds up a potential barrier at the surface of TiO₂,⁷ but it is not clear whether similar barriers are also formed at internal interfaces within the film, that is grain boundaries (GBs).⁸ Considering the fact that GBs provide easy paths for diffusion,⁹ particularly in nanocrystalline TiO₂, where the diffusion of oxygen atoms is orders of magnitude faster than in single crystals,¹⁰ it is likely that the GBs are accessible to small molecules (at elevated temperatures). Thus, chemisorption-induced barriers may also be formed at GBs inside the film. These barriers are expected to control the charge transport properties of such films in a similar manner to the GB-controlled transport in polycrystalline semiconductors,^{11,12} making them very sensitive to gas adsorption.

A correlation between the surface and GB potential barriers in polycrystalline GaN was demonstrated recently by comparing the photoinduced changes in conductivity (i.e., photoconductivity) with the surface photovoltage (SPV).¹³

Thus, surface photovoltage spectroscopy (SPS), which provides direct information on the surface electronic structure and properties of semiconductor materials,¹⁴ is also useful for investigating GB electrical properties in polycrystalline semiconductors. In this letter we present a comparative study of the electronic and transport properties of dense nanocrystalline TiO₂ (rutile) films exposed to reducing or oxidizing conditions by annealing *in vacuo* or in air, respectively, using *in situ* conductivity and *I*–*V* measurements and *ex situ* SPS measurements.

The TiO₂ films (~200 nm) were deposited on oxidized Si substrates covered with interdigital Au electrodes by reactive sputtering from a Ti target.⁵ After deposition, all samples were annealed at 450 °C in a vacuum of ~10⁻⁷ mbar for 24 h to crystallize the films and to stabilize their microstructure. *In situ* conductivity and *I*–*V* measurements were carried out in an environmental chamber⁵ at a base vacuum level of ~4×10⁻⁶ mbar and at air pressures of 1 and 10 mbar, at temperatures between 25 and 350 °C. For the *ex situ* SPS measurements, some samples were reduced (again) by annealing *in vacuo* (~10⁻⁷ mbar) at 450 °C for 24 h, and some were oxidized by annealing in dry atmospheric air at 400 °C for 24 h. The SPS measurements were conducted inside a dark Faraday cage, in atmospheric air at room temperature. The SPV was measured by monitoring changes in the contact potential difference (CPD) between the TiO₂ film and a vibrating Au reference probe using the Kelvin probe technique,¹⁴ while the sample was illuminated by monochromatic light with wavelengths between 650 and 250 nm (with 0.1 nm/s steps). The SPV is the difference between the CPD values in dark and under illumination.¹⁴ A commercial Kelvin probe apparatus (Besocke Delta Phi, Germany) was used, providing ~1 mV sensitivity. The Au electrode underneath the TiO₂ film provided common ground for the probe and sample. The samples were illuminated through a double 0.25-m grating monochromator fed by a 150-W Xe lamp. The output illumination power at the sample surface typically lay in the microwatt range, covering the entire probe area (2.5 mm in diameter). Prior to illumination, each sample

^{a)}Author to whom correspondence should be addressed; electronic mail: mtavner@tx.technion.ac.il

^{b)}Present address: The Scripps Research Institute, La Jolla, California 92037.



FIG. 1. Plan-view TEM micrograph of a typical TiO₂ film.

was maintained in the dark for 24 h in order to eliminate persisting effects of previous light exposure.

In addition to the electrical measurements, microstructural and compositional characterizations were carried out using x-ray diffraction, transmission electron microscopy (TEM), high-resolution scanning electron microscopy, and Rutherford backscattering spectroscopy (RBS). After the initial thermal treatment, the TiO₂ films had a stable nanocrystalline rutile structure that did not change upon subsequent annealing at lower temperatures.⁵ The crystallized films were columnar, as observed by cross-section TEM micrographs (not shown), with grain diameters between 10 and 80 nm (with an average of ~36 nm), as shown in the plan-view TEM micrograph in Fig. 1. RBS measurements indicated that the O/Ti ratio was about 2:1, and no impurities except for Ar (from the sputtering process) were detected.⁵

The resistance of a typical TiO₂ sample as a function of temperature at three different air pressures is depicted in Fig. 2. The first set of measurements (□) was carried out at ~4 × 10⁻⁶ mbar, after the sample had been equilibrated for ~48 h at a temperature of 350 °C until its resistance attained a steady value. Subsequently, the temperature was lowered by several steps down to 25 °C. When a steady resistance was attained at each step, the current (*I*) was measured as a function of the applied voltage (*V*) for dc biases between 0.01 and 5 V. The resistance was calculated from the slope of the *I*-*V* characteristic at the low-voltage range, where it was ohmic. A second set of measurements was similarly conducted at 1 mbar (●), and a third one at 10 mbar (▲), by

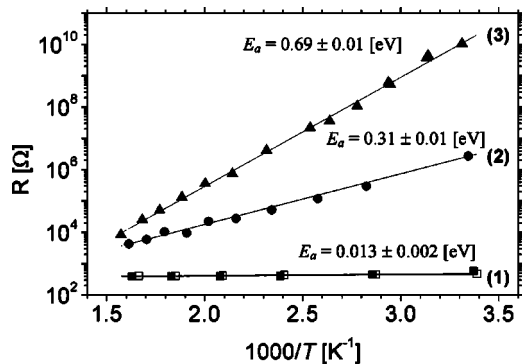


FIG. 2. Resistance as a function of the reciprocal temperature at three different air pressures: (1) at the base vacuum level, ~4 × 10⁻⁶ mbar (□ - first set, ■ - last set of measurements); (2) at 1 mbar of dry air (●); and (3) at 10 mbar of dry air (▲). *E_a* is the activation energy.

introducing dry air into the chamber (under constant flow conditions). Finally, the conditions were set back to the base vacuum level and those measurements were repeated again (■). As shown in Fig. 2, the first and last sets of measurements (at ~4 × 10⁻⁶ mbar) yielded nearly the same results, indicating that the effect of air pressure cycling was reversible.

As can be seen in Fig. 2, the ambient air pressure had a drastic effect on the resistance, changing it by almost eight orders of magnitude between the base vacuum level and 10 mbar of air (at 25 °C). In addition, the slope of the *R* versus 1/*T* curves, that is, the activation energy (*E_a*), also changed considerably from 0.01 eV at the base vacuum level to 0.31 and 0.69 eV at 1 and 10 mbar, respectively. These observations cannot be related to changes in the film structure, as it was shown to be stable after the initial thermal treatment.⁵

The resistance values depicted in Fig. 2 were measured under equilibrium conditions. According to the mass-action law, the oxygen pressure induced modifications of the TiO_{2-δ} stoichiometry lead to a power-law relationship between the resistance and the ambient oxygen pressure, $R \propto (p_{O_2})^{1/m}$, where $2 \leq m \leq 6$, depending on the predominant defects.^{15,16} Accordingly, the expected change in the resistance upon changing the air (i.e., oxygen) pressure from ~4 × 10⁻⁶ to 10 mbar cannot exceed more than three orders of magnitude, whereas Fig. 2 shows that it actually increased by nearly eight orders of magnitude (at 25 °C). Thus, the bulk oxidation effect alone is too small to account for this remarkable behavior. However, these results can be ascribed to the buildup of GB barriers induced by chemisorption of oxygen that lead to electron trapping at interface (GB) states. As a result, the resistance is $R = R_0 \exp(e|\varphi_{GB}|/kT)$, where *R*₀ is a pre-exponential coefficient that includes the bulk resistance and other factors, *e* is the elementary charge, *k* is the Boltzmann constant, *T* is the temperature, and |*φ_{GB}*| is the magnitude of the GB potential barrier.^{4,11,12} Assuming that |*φ_{GB}*| depends on the ambient oxygen pressure due to oxygen chemisorption,^{4,7,17} this relationship can explain the experimental results in Fig. 2. In addition, the *I*-*V* characteristics of the reduced film were linear (ohmic) at all the applied biases, whereas those of the oxidized film were non-linear, except at low voltages (<0.1 V). Such nonlinearity of the *I*-*V* characteristics of the oxidized film confirms the role of the GB barriers, as it is often associated with charged GBs that control the charge transport mechanism in polycrystalline semiconductors.¹⁸ In general, contact barrier effects can also lead to a similar behavior.¹⁹ However, the latter must be ruled out in the case at hand since the dark-CPD between the oxidized TiO₂ film and the Au reference electrode of the Kelvin probe was only 0.11 V. This indicates that the contact potential barrier at the TiO₂/Au interface was rather small, surely much smaller than the sum of all the GB barriers, that the current must have crossed through the film (>1000 GBs). Moreover, the resistance of the TiO₂ film scaled with the contact separation length, indicating that the film properties rather than the TiO₂/Au contacts dominated the resistance.

Figure 3 shows the SPV spectra of reduced and oxidized TiO₂ films (from the same deposition batch) as a function of the energy (*hν*) of the incident photons. The most prominent

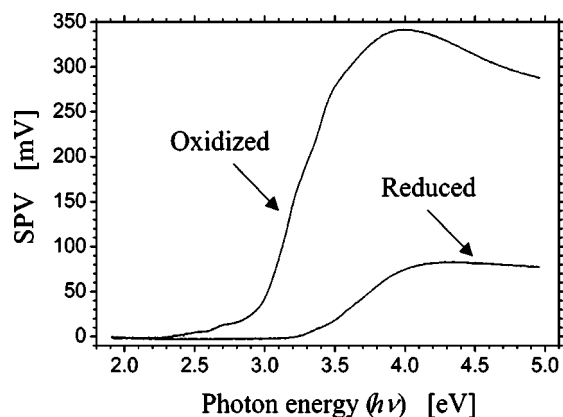


FIG. 3. SPS spectra of reduced and oxidized TiO_2 films.

difference between these spectra is the much stronger SPV signal of the oxidized film (342 mV) with respect to the reduced film (83 mV), indicating that the surface potential barrier in the former is much larger than in the latter. This is attributed to the effect of oxygen chemisorption (in the oxidized film), leading to charge transfer to surface states associated with adsorbed oxygen anions (O^- or O_2^- species).^{4,7} A similar effect probably occurred also at the GBs because charge trapping at the free surface alone is unlikely to account for the remarkable dependence of the resistance (and activation energy) on the ambient oxygen pressure. For the latter to fully account for the results shown in Fig. 2, the chemisorption-induced surface states should have captured nearly all free charges in the film, and the surface depletion layer should have covered the entire film (~ 200 nm). With an estimated Debye length between 10 and 40 nm, this is improbable. Moreover, according to the Schottky approximation for depletion layers the number of charges captured at the surface is proportional to the square root of the surface potential barrier,²⁰ which is a rather weak dependence to account for the results depicted in Fig. 2.

In conclusion, the experimental results indicate that exposure to oxygen (at 350°C) leads to the formation of a surface potential barrier and most probably also to the for-

mation of GB potential barriers that control the charge transport mechanism in those films, while annealing *in vacuo* diminishes these barriers and renders the films quite conductive. These effects are very prominent and reversible, suggesting that the films are suitable for oxygen- and gas-sensing applications, despite having a dense (rather than porous) microstructure.

The authors wish to thank Prof. F. Cosandey from Rutgers University for supplying the TiO_2 samples for this study. One of the authors (Y.S.) is grateful to D. and H. Krongold for their generous support. Another author (Y.K.) is grateful for the Fund for the Promotion of Research at the Technion for partial support.

¹M. Grätzel, *Nature (London)* **414**, 338 (2001).

²A. Fujishima and K. Honda, *Nature (London)* **238**, 37 (1972).

³A. L. Linsebigler, G. Lu, and J. T. Yates, Jr., *Chem. Rev.* **95**, 735 (1995).

⁴M. J. Madou and S. R. Morrison, *Chemical Sensing with Solid State Devices* (Academic, San Diego, 1989).

⁵A. Rothschild, F. Edelman, Y. Komem, and F. Cosandey, *Sens. Actuators B* **67**, 282 (2000); A. Rothschild, Y. Komem, and F. Cosandey, *Interface Sci.* **9**, 157 (2001).

⁶A. Rothschild, Y. Komem, and F. Cosandey, *J. Electrochem. Soc.* **148**, H85 (2001).

⁷W. Göpel, G. Rucker, and R. Feierabend, *Phys. Rev. B* **28**, 3427 (1983); W. Göpel, *Prog. Surf. Sci.* **20**, 9 (1985).

⁸N. Bàrsan and U. Weimar, *J. Electroceram.* **7**, 143 (2001).

⁹I. Kaur, Y. Mishin, and W. Gust, *Fundamentals of Grain Boundary Diffusion* (Wiley, Chichester, 1995).

¹⁰H. J. Höfler, H. Hahn, and R. S. Averback, *Defect Diffus. Forum* **75**, 195 (1991).

¹¹J. Y. W. Seto, *J. Appl. Phys.* **46**, 5247 (1975).

¹²G. E. Pike and C. H. Seager, *J. Appl. Phys.* **50**, 3414 (1979).

¹³I. Shalish, L. Kronik, G. Segel, Y. Shapira, S. Zamir, B. Meyler, and J. Salzman, *Phys. Rev. B* **61**, 15573 (2000).

¹⁴L. Kronik and Y. Shapira, *Surf. Sci. Rep.* **37**, 1 (1999); *Surf. Interface Anal.* **31**, 954 (2001).

¹⁵J. Nowotny, M. Radecka, and M. Rekas, *J. Phys. Chem. Solids* **58**, 927 (1997).

¹⁶P. Knauth and H. L. Tuller, *J. Appl. Phys.* **85**, 897 (1999).

¹⁷P. R. Bueno, E. R. Leite, M. M. Oliveira, M. O. Orlandi, and E. Longo, *Appl. Phys. Lett.* **79**, 48 (2001).

¹⁸F. Greuter and G. Blatter, *Semicond. Sci. Technol.* **5**, 111 (1990).

¹⁹R. van de Krol and H. L. Tuller, *Solid State Ionics* **150**, 167 (2002).

²⁰W. Mönch, *Semiconductor Surfaces and Interfaces*, 3rd ed. (Springer, Berlin, 2001).